

# Theoretical and Experimental Investigations of the Corrosion Inhibition Action of *Piliostigma Thonningii* Extract on Mild Steel in Acidic Medium

\*Paul Ocheje Ameh and Nnabuk Okon Eddy

Received 05 July 2018/Accepted September 2018/Published online: 4 December 2018

**Abstract** The search for green corrosion inhibitor for mild steel in solution of HCl was implemented in this work by using electrochemical polarization, gravimetric and thermometric techniques to ascertain the corrosion inhibition efficiency of ethanol extract of *Piliostigma thonningii* leaf. Weight loss and thermometric measurements indicated the inhibition efficiency of ethanol extract of *Piliostigma thonningii* leaf to range from 65.12 to 79.55 % and from 73.61 to 88.16 % respectively. Inhibition efficiencies obtained from, linear and potentiodynamic polarization measurements gave the ranges, 66.40 to 89.97 % and 51.29 to 85.53 % respectively. Active components of the extracts that synergistically cooperate to enhance their adsorption on mild steel surface (and hence corrosion inhibition) were identified through GCMS analysis and they included 1,1,7-trimethyl-4-methylenedecahydro-1H-cyclopropa[e]azulene; hydroquinone; 3-tridecene; 3,5-bis(1,1-dimethylethyl)-phenol; Pentadecanoic acid; 1-ethenyl-1-methyl-2,4-bis(1-methylethenyl)-cyclohexane and 9-oxa-bicyclo[3,3,1]nona-3,6-dien-2-one. Quantum chemical calculations revealed that these compounds, apart from meeting the basic requirements for corrosion inhibition, they are also characterized by frontier molecular energy values that are unique for well-known corrosion

**N. O. Eddy**

Department of Pure and Applied Chemistry  
University of Nigeria, Nsukka, Enugu State,  
Nigeria

Email: [okon.nnabuk@unn.edu.ng](mailto:okon.nnabuk@unn.edu.ng)

## 1.0 Introduction

Mild steel (among metals), is widely applied in several industrial installations due to some of its unique parameters (Eddy *et al.*, 2009a). However, the metal is highly prone to corrosion when exposed to aggressive medium such as those that are used for acid cleaning, etching, descaling, crude oil/crude oil products transportation, transportation of fertilizers and fertilizer chemicals, etc (Ameh and Eddy, 2014). Efforts in reducing damages due to corrosion have resulted in different control options including electroplating, cathodic/anodic protections, greasing/oiling among others. However, it has been established that the use of corrosion inhibitors is the best and unique option of retarding metal corrosion, especially those accelerated by aggressive medium (Eddy *et al.*, 2010). Different compounds have been found to be active corrosion inhibitors ranging from some inorganic compounds, drugs, polymers, Schiff bases, molecular liquids, nano materials, plant materials and others (Awe *et al.*, 2019; Anand and Chitra, 2020; Azzan *et al.*, 2019; Eddy *et al.*, 2011; Eddy *et al.*, 2009b; Saravanan and Yadav, 2020;

er, in spite of their high corrosion inhibition efficiencies, most of them have some setbacks in meeting environmental and other requirements including biodegradability, less cost, less toxicity, ease of availability and eco friendliness (Eddy and Odiongenyi, 2010; Lebrini *et al.*, 2008; Umoren *et al.*, 2008). Therefore, several hopes have been laid on the use of extracts of living things since most of

**Key Words:** Mild steel, corrosion inhibition, *Piliostigma thonningii* leaf, experimental and theoretical considerations

\*P. O. Ameh

Physical Chemistry Unit, Department of Chemistry  
Nigeria Police Academy, Wudil, P. M B. 3474,  
Kano State Nigeria

E-mail: [amehpaul99@gmail.com](mailto:amehpaul99@gmail.com)

them can meet these requirements. Products of plant origin contain various organic compounds such as alkaloids, flavonoids, terpenoids, primary and secondary alcohols, quinones, fatty acids, steroids and other minor components (Adejo *et al.*, 2012; Akalezi *et al.*, 2012; Eddy, 2009; Eddy and Ebenso, 2008; Oguzie, 2008; Edeoga *et al.*, 2005; Nwosu *et al.*, 2013). The use of GCMS in providing information on the major phytochemicals in plant extract used for corrosion studies has been advocated by several authors (Arthur, 2020; Karunanithi & Chellappa, 2019; Yinusa and Raphael, 2020; Jimoh and Oladii, 2005). The choice of corrosion monitoring techniques is significant in drawing conclusions from corrosion study. Generally, gravimetric method is unique in providing data for average corrosion rate and inhibition efficiency while other methods (including polarization, electrochemical impedance spectroscopy, gasometric, etc) also have their own unique advantages but they provide information on instantaneous corrosion rate. Information on corrosion current, corrosion voltage, mechanism of inhibition and type of inhibition can be obtained from polarization method. One of the recent approaches to corrosion inhibition has been the use of computational chemistry to proposed adsorption models for corrosion inhibition by plant extracts (Arthur, 2020; Eddy and Ita, 2011; Eddy *et al.* 2011).

Excessive limited information is available on the corrosion inhibition studies have been reported for ethanol extract of *Piliostigma thonningii* leaf but they are all deplete of exhaustive work. Kobe *et al.* (2011) used gravimetric, gasometric, GCMS and FTIR techniques. The results indicated good inhibition efficiencies but electrochemical method was not incorporated to the study hence experimental mechanistic models couldn't be activated in the study and quantum chemical or theoretical projection was not also possible. Similar reasons have also shortened information from the work reported by Onen *et al.* (2017). *Piliostigma thonningii* leaf is nontoxic edible leaf (Burkill, 1995) and is biodegradable. Therefore, present study is aimed at investigating the inhibition potential of ethanol extract of *Piliostigma thonningii* leaf for the inhibition of mild steel corrosion in solution of HCl

using gravimetric, gasometric, GCMS and computational chemistry methods.

## 2.0 Materials and Methods

### 2.1. Materials

Mild steel sheet of composition (weight %) C (0.15), Mn (0.62), P (0.38), and Si (0.03) and Fe (98.85) was used for the study. The sheet was cut into two sets of coupons, with different dimensions, namely  $2 \times 1.5 \times 0.05$  cm and  $5 \times 4 \times 0.05$  cm for used in electrochemical and weight loss (and thermometric) experiments respectively. Each coupon was polished with series of emery paper of variable grades starting with the course (400 grade) and then proceeding in steps to the finest (1200) grades. The polished coupons were washed with distilled water, rinsed with absolute ethanol, cleaned in acetone and allowed to dry in the air before being preserved in a desiccator. All reagents were analar grade supplied by BDH chemicals, England.

### 2.2. Extraction of plants

Samples of *Piliostigma thonningii* leaves were obtained from Ningi Local government of Bauchi State Nigeria. It was taken to Herbarium in Department of Biological Sciences, Bayero University Kano State for identification and assignment of batch number. The leaves were dried, grounded and soaked in a solution of ethanol for 48 hours. The filtrate obtained after 48 hours was subjected to evaporation at 352 K in order to leave the sample free of ethanol. The stock solution obtained from the ethanol extract was used in preparing different concentrations of the extract (0.1, 0.2, 0.3, 0.4, and 0.5 g/L) through serial dilution.

### 2.3 GC-MS analysis

GC-MS investigation of ethanol extract of *Piliostigma thonningii* leaf was conducted at National Institute of Chemical Technology (NARICT), Zaria, Nigeria using a Shimadzu QP2010 plus series gas chromatography coupled with Shimadzu QP2010 plus mass spectroscopy detector (GC-MS) system. Interpretation on mass spectrum GC-MS was conducted using the database of National Institute Standard and Technology (NIST) Abuja, having more than 62,000 patterns. The spectrum of the unknown component was compared with the spectrum of the known components stored in the NIST library. The name, molecular weight and structure of the components of



the test materials were ascertained. The concentrations of the identified compounds were determined through area and height normalization.

#### 2.4 Gravimetric (weight loss) method

Weight loss measurements were carried out in line with ASTM practices standard G-31 (2004). The experiment was carried at 303 K, 313 K, 323 K and 333 K. The average weight loss of the specimens in the presence and absence of studied inhibitor system were taken and the corrosion rate (CR), degree of surface coverage ( $\theta$ ) and the inhibition efficiency (% I) of the inhibitor were calculated using equations 1, 2 and 3 respectively Ameh (2018).

$$\text{Corrosion rate (CR)} = \frac{534W}{DAT} \quad (1)$$

$$\theta = \left(1 - \frac{W_1}{W_2}\right) \quad (2)$$

$$\%I = \left(1 - \frac{W_1}{W_2}\right) \times 100 \quad (3)$$

where W is the weight loss (mg); D is density of specimen ( $\text{g/cm}^3$ ), A is area of specimen (square centimeters), T is the period of immersion of the metal (hour),  $W_1$  and  $W_2$  are the weight losses ( $\text{g/dm}^3$ ) for the mild steel in the presence and absence of inhibitor in the corrodent respectively.

#### 2.5 Thermometric method

This was also carried out as reported by Eddy and Ebenso (2008). A three-neck flask with provisions for the introduction of chemicals and for insertion of thermometer was used for thermometric study. For each study, the mild steel coupon was introduced into the flask. Enough quantities of each solution were in turn transferred into the flask until the metal coupons were completely immersed. Once this was done, the temperature of the reacting solution was read at one-minute interval until a constant temperature was obtained. The reaction number (RN) of each system was calculated by dividing the difference between the highest and lowest temperature attained by the time interval. From the reaction number, the inhibition efficiency (% I) of the inhibitor was calculated using the equation 4 (Eddy and Ebenso, 2008).

$$I = \frac{RN_{aq} - RN_{wi}}{RN_{aq}} \times \frac{100}{1} \quad (4)$$

where  $RN_{aq}$  is the reaction number in the absence of inhibitors and  $RN_{wi}$  is the reaction number in the presence of the inhibitor.

#### 2.6 Electrochemical study

Electrochemical tests were carried out as described by Quraishi and Singh Quraishi (2010) using a

rectangular coupon embedded in resin plastic mounted with an exposed surface of  $165 \text{ mm}^2$ . The electrode was polished with different grades of silicon carbide paper, rinsed with distilled water and dried with acetone. The studies were performed at ambient temperature with a potentiostat (Autolab PGSTAT 30 ECO CHIMIE) and an electrode cell containing  $200 \text{ cm}^3$  of electrolyte, with and without the inhibitor. A saturated calomel electrode (SCE) and a platinum electrode were used respectively as reference and auxiliary electrode. To attain constant steady state, the electrode was immersed in the test solution for a minimum of half an hour before taking electrochemical measurements. The polarization studies were carried out in the potential range of  $\pm 250 \text{ mV}$  for mild steel and in the potential range of  $-1000$  to  $2000 \text{ mV}$  for aluminium at a scan rate of  $0.5 \text{ mV s}^{-1}$ . Each test was run in triplicate. In Potentiodynamic polarization (PDP), the linear Tafel segments of the anodic and cathodic curves obtained were extrapolated to corrosion potential to obtain the corrosion current densities ( $i_{\text{corr}}$ ). The inhibition efficiency (I %) was evaluated from the measured  $i_{\text{corr}}$  values<sup>XX</sup>.

$$\%I = \frac{i_{\text{Corr}}^0 - i_{\text{Corr}}}{i_{\text{Corr}}^0} \times \frac{100}{1} \quad (5)$$

where  $i_{\text{Corr}}^0$  and  $i_{\text{Corr}}$  are the uninhibited and inhibited corrosion current densities, respectively. For linear polarization resistance (LPR), the potential and current data was plotted on a linear scale to get LPR plots, and the slope of the plots in the vicinity of the corrosion potential gave the polarization resistance ( $R_p$ ). From the measured  $R_p$  values, the inhibition efficiency (I %) was calculated using equation 6 (Benabdellah *et al.*, 2007).

$$\%I = \frac{R_{p(\text{inh})} - R_p}{R_{p(\text{inh})}} \times \frac{100}{1} \quad (6)$$

where  $R_p$  and  $R_{p(\text{inh})}$  are the polarization resistances for uninhibited and inhibited system respectively.

#### 2.7 Quantumr dynamics simulation study

Molecular dynamics (MD) simulation of the interactions between the inhibitor molecules identified from GCMS studies and Fe surface was performed using Forcite quench molecular dynamics in the Material Studio (MS) modelling 7.0 software. Calculations were carried out using COMPASS forcefield and Smart algorithm in a simulation box  $17 \text{ \AA} \times 12 \text{ \AA} \times 28 \text{ \AA}$  with a periodic boundary condition, to model a representative part of the Fe slab and a vacuum layer of  $20 \text{ \AA}$  height.



The Fe crystal was cleaved along the (110) plane with a fractional depth of 3.0 Å. The geometry of the bottom layers was constrained before optimizing the Fe (110) surface which was subsequently enlarged into a 10 x 9 supercell to avoid edge effects. Temperature was fixed at 350 K with the NVE (microcanonical) ensemble with a time step of 1 fs and simulation time 5 ps. The system is quenched every 250 steps. Forcite optimised structures of the constituents from the studied plant extracts compounds and the Fe surface was used to sample the different interactions of the molecule with the surfaces. The slab of Fe constructed for the docking was significantly bigger than the compounds docked in order to avoid edge effects.

### 3.0 Results and Discussion

#### 3.1. GC-MS study

GCMS spectrum ethanol extract of *Piliostigma thonningii* leaf is shown in Fig. 1. Information deduced from the spectrum (Table 1) were retention time, molecular formula, mass peaks, fragmentation peaks and percentage concentration (obtained from height and area normalization). From spectrum, it is evident that seven peaks were observed and the corresponding compounds are recorded in Table 1. The chemical structures of identified compounds are shown in Fig. 2. From

the structures, it is evident that all the identified compounds ( viz,  $\pm$ hydroquinone; 3-tridecene, 3,5-bis(1,1-dimethylethyl)-pheno, pentadecanoic acid, 1-ethenyl-1-methyl-2,4-bis(1-methylethenyl)-

**Table 1: Parameters deduced from GC-MS spectrum of ethanol extract of *Piliostigma thonningii*(PT) leaf**

Compound	C (%)	Chemical formula	RT (s)	MW (g/mol)	Fragmentation Peak
Hydroquinone	8.91	C <sub>6</sub> H <sub>6</sub> O <sub>2</sub>	8.11	110	26(16%), 40(19%), 54(16%), 55(23%), 81(40%), 82(21%), 98(100%)
3-tridecene	3.56	C <sub>13</sub> H <sub>26</sub>	11.32	182	25(23%), 35(45%), 37(21%), 43(60%), 54(11%), 57(56%), 59(33%), 63(20%), 69(41%), 72(43%), 78(20%), 85(95%), 89(68%), 98(62%)
3,5-bis(1,1-dimethylethyl)-phenol	28.99	C <sub>14</sub> H <sub>22</sub> O	12.44	206	41(14%), 57(65%), 58 (70%), 59(22%), 66(42%) 80(20%), 88(18%), 90(70%)

cyclohexane; 9-oxa-bicyclo[3,3,1]nona-3,6-dien-2-one and 1,1,7-trimethyl-4-methylenedecahydro-1H-cyclopropa[e] -azulene) meets the requirements to be a good corrosion inhibitors including possession of aromatic system,  $\pi$ -bond, conjugated bond, heteroatoms and long carbon chains (Ameh, 2018; Karunanithi and Chellappa, , 2019). Therefore, this extract can be viewed as compound that has several corrosion inhibitors.

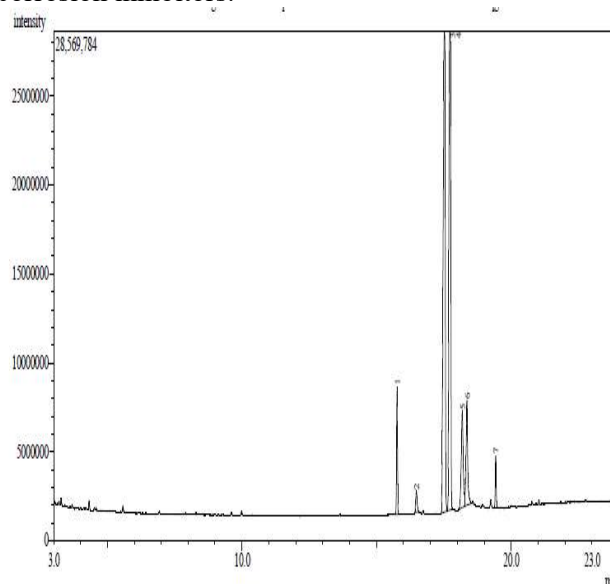


**Fig. 1: GC-MS spectrum of ethanol extract of *Piliostigma thonningii***



<b>Pentadecanoic acid</b>	31.54	C <sub>17</sub> H <sub>34</sub> O <sub>2</sub>	15.43	270	25(11%), 32(28%), 39(35%), 44(28%), 53(21%), 62(100%), 70(52%), 75(29%), 81(40%), 110(43%), 125(25%), 126(22%), 128(18%)
<b>1-ethenyl-1-methyl-2,4-bis(1-methylethenyl)-cyclohexane</b>	11.68	C <sub>15</sub> H <sub>24</sub>	10.16	204	22(24%), 30(31%), 40(15%), 43(27%), 45(70%), 47(33%), 50(22%), 53(34%), 58(80%), 60(22%), 61(24%), 63(20%), 65(15%), 67(56%), 70(33%), 73(23%), 76(40%), 78(20%), 80(99%), 93(44%), 95(63%), 99(86%), 100(70%), 111(15%), 123(28%), 130(43%), 141(12%), 151(34%)
<b>1,1,7-trimethyl-4-methylenedecahydro-1H-cyclopropa[e]azulene</b>	13.72	C <sub>15</sub> H <sub>24</sub>	11.32	204	28(34%), 29(22%), 32(34%), 43(91%), 47(23%), 51(22%), 54(28%), 60(23%), 68(13%), 71(33%), 76(33%), 80(42%), 81(17%), 93(86%), 94(100%), 99(45%), 102(43%), 105(44%), 110(100%), 118(46%), 128(27%), 131(44%), 142(52%), 154(77%)
<b>9-oxa-bicyclo[3,3,1]nona-3,6-dien-2-one</b>	1.60	C <sub>8</sub> H <sub>18</sub> O <sub>2</sub>	8.16	138	26(25%), 28(22%), 46(55%), 50(52%), 52(42%), 62(42%), 68(70%), 71(32%), 88(100%), 102(22%), 103(11%)

\*\* C = concentration, MW = molecular weight, T = retention time, \*\* compounds are arranged to match the peak number

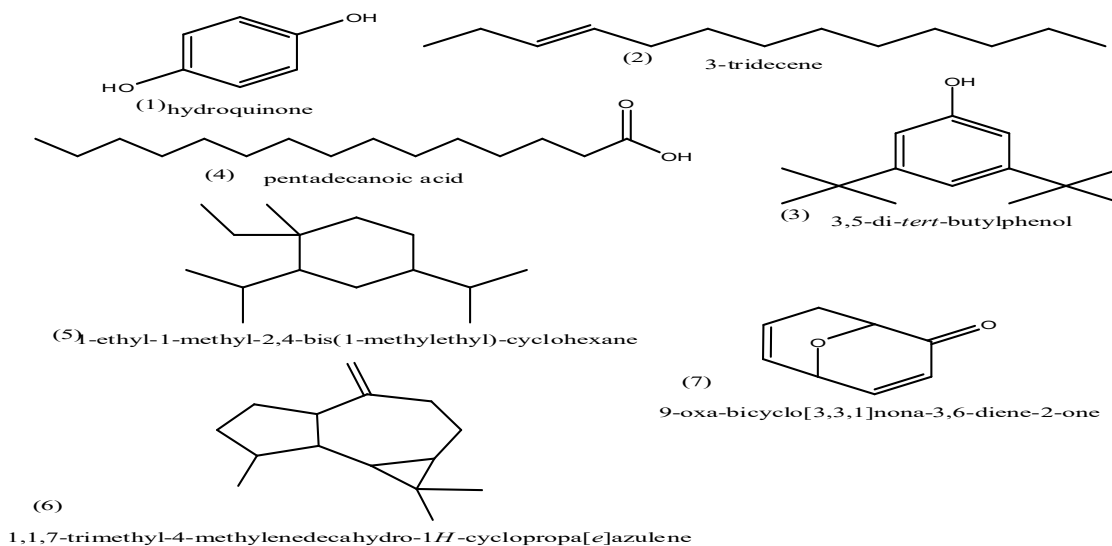




**Fig. 2: Chemical structures of compounds identified by GCMS of ethanol extract of *Piliostigma thonningii*(PT) leaf**

**3.2 Gravimetric and thermometric studies**

Plots showing the variation of weight loss with time for the corrosion of mild steel in 0.1 M HCl at

303 to 333 K in the absence and presence of various concentrations of ethanol leave extract of PT are shown in Fig. 3.

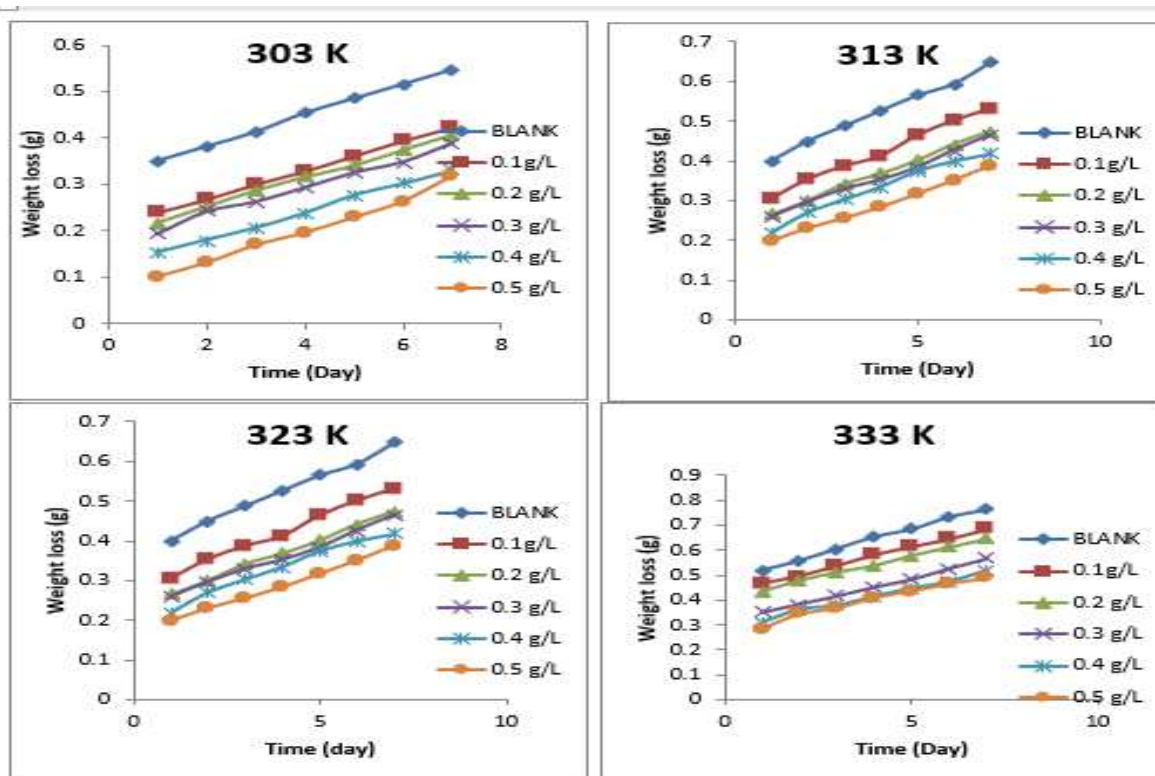


**Fig. 3: Variation of weight loss with time for the corrosion of mild steel in 0.1 M HCl containing (0.1 to 0.5 g/L) ethanol extract of PT leaf.**

The Figures reveal that weight loss of mild steel, hence corrosion rate (Table 2), increases with time and with temperatures, which translate to a decrease in inhibition efficiency with time and temperature. It also implies that the extent of adsorption of ethanol extract of PT leaf decreases

with temperature, a trend that is obvious for physisorption mechanism (Adejo *et al.*, 2012). Calculated inhibition efficiency and corrosion rates for various concentrations of ethanol extract of PT leaf are also presented in Table 2.

**Table 2: Corrosion rate and inhibition efficiency of various concentrations of *Piliostigma thonningii* for mild steel from gravimetric and thermometric measurement**

C (g/L)	Corrosion rate ( $\text{g m}^{-2} \text{h}^{-1}$ )				$I_G$ (%)				$I_T$ (%)
	303 K	313 K	323 K	333 K	303 K	313 K	323 K	333 K	303 K
Blank	0.01378	0.01998	0.03015	0.03889	-	-	-	-	-
0.1	0.00811	0.01729	0.02354	0.03350	65.12	47.25	38.80	26.84	73.64
0.2	0.00610	0.01414	0.02108	0.03316	68.66	45.78	40.94	31.20	77.91
0.3	0.00462	0.01114	0.01978	0.03128	72.85	54.10	41.65	33.25	79.22
0.4	0.00354	0.00943	0.01923	0.02796	76.61	58.59	42.05	35.55	84.09
0.5	0.00275	0.00859	0.01859	0.02685	79.55	62.64	47.24	44.87	88.46



**\*\*I<sub>G</sub> = Inhibition efficiency from gravimetric method, I<sub>T</sub> = Inhibition efficiency from thermometric method**

Inhibition efficiency from both gravimetric and thermometric methods are seen to increase with increase in concentration but decreased with increasing temperature. Therefore, the extract enhances corrosion inhibition as its concentration increases but its efficiency is retarded by increase in temperature and in the period of contact. This may be due to denature of the extract's active components at higher temperature. Such denaturation will reduce the rate of adsorption and thus decrease inhibition efficiency. Inhibition efficiencies from thermometric and gravimetric methods correlated strongly ( $R^2 = 0.9593$ ), which also validate the two experimental methods. However, higher values were observed for thermometric data compared with those obtained from gravimetric measurements. This is explained with reference to the period of contact the metals remain in the aggressive medium since corrosion rate increase with increase in the period of contact. Consequently, thermometric measurement described instantaneous corrosion measurements unlike gravimetric experiments, which measures average corrosion inhibition. Similar findings have been reported elsewhere (Eddy *et al.*, 2011)

**3.3 Electrochemical study**

Fig. 4 shows potentiodynamic polarization plots of the corrosion of mild steel in 0.1 M HCl in the presence of various concentrations of PT extract at 303 K. Corrosion kinetic data (including corrosion current density ( $i_{corr}$ ), corrosion potential ( $E_{corr}$ ), anodic ( $\beta_a$ ) and cathodic ( $\beta_c$ ) Tafel constants) and calculated inhibition efficiencies are also presented in Table 3. Increase in corrosion current is an index for increase in corrosion rate and from the results presented, the corrosion current was observed to decrease with increase in concentration of ethanol

extract of PT leaf indicating that electrochemical polarization data also confirmed that ethanol extract of PT leaf is an adsorption inhibitor because its inhibition efficiency increase with increase in concentration (Quraishi and Singh Quraishi, 2010). This finding is also similar from weight loss and gravimetric data. Remarkable changes were not observed in the magnitude of Tafel anodic ( $\beta_a$ ) and cathodic ( $\beta_c$ ) constants with increasing extract concentration. This suggests that the inhibitor is not interfering with the cathodic hydrogen evolution reactions or anodic dissolution independently but acted synergistically, which is a feature of a mixed type of inhibitor (Benabdellah *et al.*, 2007).

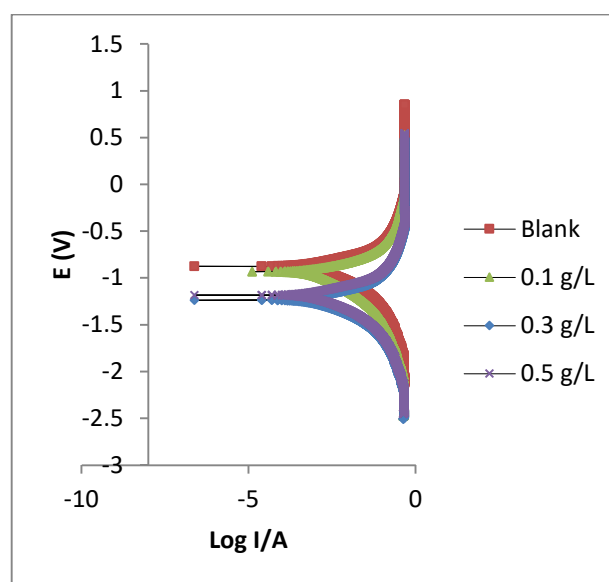


**Fig 4: Potentiodynamic polarization curves for the Mild steel in 0.1 M HCl in the absence and presence of different concentrations of PT**

**Table 3: Polarization data for the corrosion of mild steel in 0.1 M HCl in the absence and presence of PT at 303 K**

C (g/L)	Linear Polarization Resistant		Potentiodynamic Polarization				
	R <sub>p</sub> (Ω / cm <sup>2</sup> )	% I	β <sub>a</sub> mVdec <sup>-1</sup>	β <sub>c</sub> mVdec <sup>-1</sup>	E <sub>corr</sub> (mV)	I <sub>corr</sub> (μA)	I %
Blank	22.32	-	128.6	133.5	- 590	104.71	-
0.1	66.43	66.40	114.6	110.8	- 571	51.00	51.29
0.3	101.26	77.96	105.0	107.4	- 548	19.64	81.24
0.5	222.61	89.97	102.3	105.9	- 535	15.15	85.53



Linear polarization measurements yielded data that (also recorded in Table 3) that were also used to calculate inhibition efficiency. Increase in polarization resistant as the extract concentration increases indicates that the corrosion of mild steel was increasingly retarded with increase in concentration of ethanol extract of PT leaf. This corresponded to increase in corrosion inhibition efficiency with increasing temperature as remarked from other methods. Correlation between linear and potentiodynamic polarization inhibition efficiency was excellent ( $R^2 = 0.8342$ ) and created no serious doubt on the precision of the two sets of experimental data.

### 3.3 Effect of temperature

Effect of temperature on the corrosion of mild steel was explained using the Arrhenius equation which related the activation energy to temperature according to equation 7 (Hassan and Sadek, 2014).

$$\ln CR = \frac{-E_a}{RT} + \ln(A) \quad (7)$$

$E_a$  is the activation energy,  $A$  is the Arrhenius or pre-exponential factor,  $R$  is the gas constant and  $T$  is the temperature. A plot of  $\ln(CR)$  versus  $1/T$  for the adsorption of ethanol extract of PT leaf on mild steel is shown in Fig. 5.

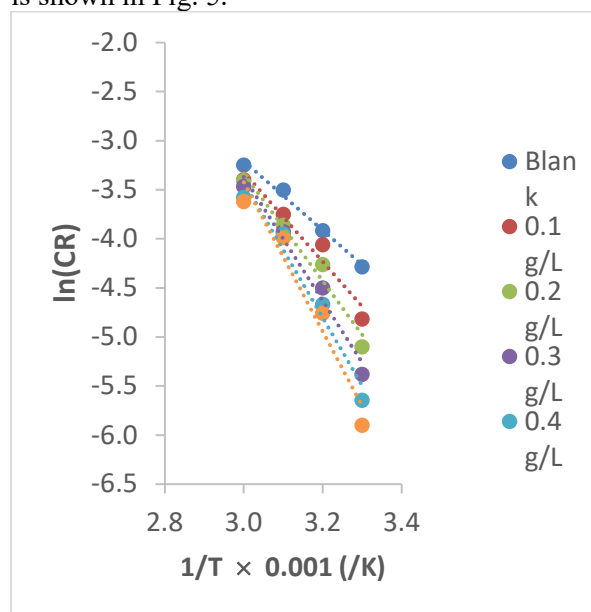


**Fig. 5: Variation of  $\ln(CR)$  with  $1/T$  for the adsorption of ethanol extract of PT leaf on mild steel surface**

Activation energy and pre-exponential factors obtained from the plots are presented in Table 4. The results show that the activation energy for the blank

is less than those obtained in the presence of the inhibitor, indicating that the inhibitor retarded the corrosion of mild steel through adsorption. Also, the activation energy increases with increase in the inhibitor's concentration indicating that the strength of adsorption of the inhibitor also increase with increase in its concentration. Although the significant of the pre-exponential factor has not fully been explored in corrosion study, it is obvious that it is related with the degree of disorderliness of the system (if the Arrhenius equation is compared with the Transition state equation). Therefore, for the same reason, the observed trend in variation of pre-exponential factor with concentration indicates that there is increasing degree of association with increasing concentration.

**Table 4: Arrhenius parameters for adsorption of ethanol extract of PT leaf on mild steel surface**

C (g/L)	Slope	ln(A)	Ea (J/mol)	R <sup>2</sup>
0.1 M HCl	-3.523	7.3641	29.29	0.9914
0.1	-4.5639	10.372	37.94	0.9516
0.2	-5.4785	13.101	45.55	0.9679
0.3	-6.3119	15.567	52.48	0.9773
0.4	-6.963	17.316	57.89	0.9630
0.5	-7.608	19.401	63.25	0.9511

### 3.4 Thermodynamic and adsorption studies

Thermodynamic parameters for the adsorption of ethanol extract of PT leaf on mild steel were calculated using the Transition state equation, which can be written according to equation 8 (Loto *et al.*, 2014; Momoh-Yahaya *et al.*, 2014),

$$CR = \frac{RT}{Nh} \exp\left(\frac{\Delta S_{ads}^*}{R}\right) \exp\left(\frac{-\Delta H_{ads}^*}{RT}\right) \quad (8)$$

Simplification of equation 8 leads to the linear form of the Transition state equation as follows,

$$\ln\left(\frac{CR}{T}\right) = \left\{ \ln\left(\frac{R}{Nh}\right) + \frac{\Delta S_{ads}^*}{R} \right\} - \frac{\Delta H_{ads}^*}{RT} \quad (9)$$

Enthalpy and entropy changes were obtained from the slope and intercept of the Transition state plots (i.e. a plot of  $\ln\left(\frac{CR}{T}\right)$  versus  $1/T$ ) shown in Fig. 6.

Thermodynamic adsorption parameters calculated from the slope and intercept of the plots are recorded in Table 5. The enthalpy changes are positive and increases with increase in concentration of the inhibitor indicating that the adsorption is endothermic and the heat of adsorption increases





with increasing inhibitor's concentration while the entropy changes are negative and decrease with increase in concentration of the inhibitor, indicating increasing degree of association of the inhibitor molecules with increasing concentration.

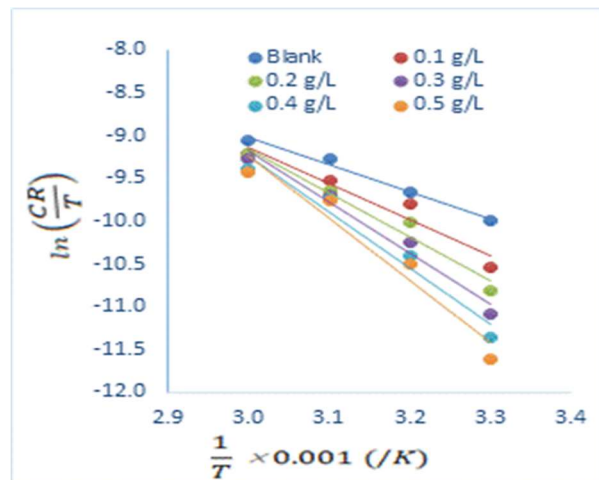


**Fig. 6:** Variation of  $\ln\left(\frac{CR}{T}\right)$  with  $\frac{1}{T}$  for the adsorption of ethanol extract of PT leaf on mild steel surface

**Table 5:** Thermodynamic parameters for the adsorption of ethanol extract of PT leaf on mild steel surface.

C (g/K)	Slope	Intercept	$\Delta H_{ads}^*$ (J/mok)	$\Delta S_{ads}^*$ (J/mok)	R <sup>2</sup>
0.1 M HCl	-3.2093	0.6114	26.68	-192.454	0.9899
0.1	-4.2492	3.6193	35.33	-167.446	0.945
0.2	-5.1638	6.3485	42.93	-144.756	0.9642
0.3	-5.9972	8.8141	49.86	-124.257	0.9751
0.4	-6.5078	10.563	54.11	-109.717	0.9597
0.5	-7.2933	12.649	60.64	-92.3735	0.9473

Increase in inhibition efficiency of ethanol extract of PT with concentration confirms that the inhibitor is an adsorption inhibitor (Monika and Dubey, 2005). The characteristics of the adsorption process associated with the inhibition can be expounded using adsorption isotherms. Various adsorption isotherms are known but the isotherms that best describe the adsorption of ethanol extract of PT leaf were Langmuir and Frumkim adsorption isotherms. The Langmuir adsorption model can be expressed in a logarithm form as follows (Zhang and Hua, 2009),

$$\ln\left(\frac{C}{\theta}\right) = \ln k_{ads} - \ln C \quad (10)$$

where C is the concentration of the inhibitor in the bulk solution,  $\theta$  is the degree of surface coverage,  $k_{ads}$  is the Langmuir equilibrium constant. The requirement that plotting of  $\ln\left(\frac{C}{\theta}\right)$  versus  $\ln(C)$  should be linear is consistent with the Langmuir model (equation 10). The Langmuir isotherm for adsorption of ethanol extract of PT leaf is shown in Fig. 7. The ideal Langmuir adsorption model assumes that there is no interaction between the adsorbed species and where interactions exist, the slope will not be equal to unity (as expected from equation 10).

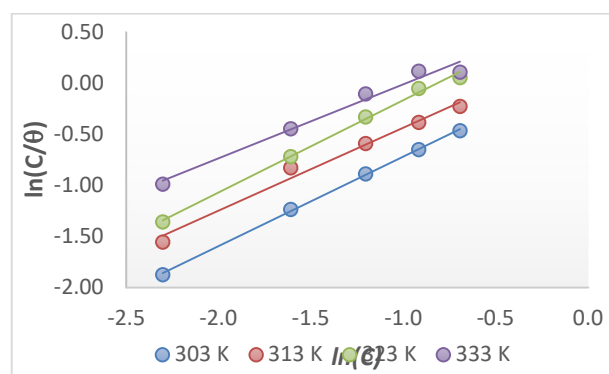


**Fig. 7:** Langmuir isotherm for adsorption of ethanol extract of PT on mild steel surface

**Table 6:** Langmuir parameters for adsorption of PT on mild steel

T(K)	Slope	$\ln k_{ads}$	$\Delta G_{ads}$ (kJ/mol)	R
303	0.875	0.1552	-13.63	0.9993
313	0.8121	0.3768	-14.35	0.9853
323	0.9018	0.712	-15.45	0.9960
333	0.7239	0.7343	-15.52	0.9775

Calculated slope values and other Langmuir parameters presented in Table 6 reveal that the slopes are very close to unity (ranging from 0.9975 to 0.99930). Therefore, there is little or no interaction between the adsorbed species. The results shows that the Langmuir adsorption equilibrium constant tend to increase with increase in concentration of ethanol extract of PT leaf indicating increasing ease of adsorption with increase in the inhibitor's concentration



The linear form of the Frumkin adsorption isotherm can be written according to equation 11 (Akinbulumo *et al.*, 2020)

$$\ln \left[ (C) \left( \frac{\theta}{1-\theta} \right) \right] = 2\alpha\theta + \ln k_{ads} \quad (11)$$

Therefore, when values of  $\ln \left[ (C) \left( \frac{\theta}{1-\theta} \right) \right]$  is plotted against  $\theta$ , obedient of adsorption data to the Frumkin adsorption model yields slope and intercept values of  $2\alpha$  and  $\ln k_{ads}$  respectively. Frumkin plots for the adsorption of ethanol extract of PT leaf is shown in Fig. 8.

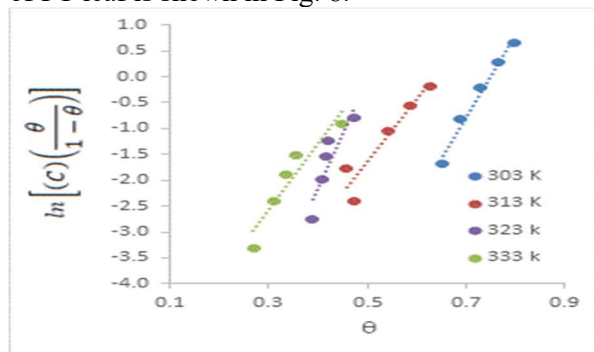


**Fig. 8: Frumkin isotherm for adsorption of ethanol extract of PT leaf on mild steel surface**

Frumkin adsorption parameters are recorded in Table 7. The results infer that the lateral interaction parameters are positive, which indicate attractive behaviour of the inhibitor's molecules.

The equilibrium constant of adsorption calculated from the intercept of the isotherms was used to calculate the standard free energy of adsorption using equation 8 (Abd El-Rehim *et al.*, 2004).

$$\Delta G_{ads}^* = -RT \ln(55.5 k_{ads}) \quad (8)$$

Calculated free energy change were found to increase with increase in concentration and ranged from -13.65 to -15.52 kJ/mol. Those obtained from Frumkin adsorption constants were also negative and were within the same range. Therefore, the adsorption of ethanol extract of PT leaf on mild steel surface is spontaneous and supports the mechanism of physical adsorption (Banumathi *et al.*, 2010).

### 3.5 Computational study

According to the frontier molecular orbital theory, the reactivity of a chemical specie is a function of the interaction of the energies of the highest Increase in the HOMO energy favours the donation of electron to vacant d-orbital of the metal while occupied molecular orbital ( $E_{HOMO}$ ) and that of the LUMO ( $E_{LUMO}$ )(Eddy, 2010). decreasing value of

the LUMO energy favours acceptance of electron from the donor. Consequently, adsorption is favourable when the energy of the HOMO increases and that of the LUMO decrease (Khalil, 2003).

**Table 7: Frumkin adsorption parameters for adsorption of ethanol extract of PT unto mild steel surface**

T (K)	Slope	$\ln k_{ads}$	$\alpha$	$\Delta G_{ads}$ (kJ/mol)	$R^2$
303	15.733	-11.772	7.87	-19.54	0.9828
313	11.859	-7.5604	5.93	-8.93	0.8941
323	21.409	-10.684	10.70	-16.80	0.7978
333	12.872	-6.4237	6.44	-6.06	0.8952

The difference between the energies of the LUMO and that of the HOMO is the energy gap of the molecule. Influence of the energy gap on adsorption of a corrosion inhibitor can be interpreted by the hard-soft molecule theory which specified that soft molecules are more reactive than hard molecule because the gap needed for the transfer and acceptance of electron is smaller. Therefore, adsorption favour lower energy gap than larger ones. Calculated frontier molecular orbital energies of the identified compounds in ethanol extract of PT leaf are presented in Table 8.

It is interesting to note that some of the compounds identified in the GCMS of ethanol extract of PT leaf have been confirmed to be good corrosion inhibitors. Sherine *et al.* (2010) reported that hydroquinone in combination with  $Zn^{2+}$  inhibited the corrosion of carbon steel with inhibition efficiency up to 97 %. However, Otieno *et al.* (1993) reported that hydroquinone enhances the pitting corrosion behaviour of A-470 low alloy turbine disc steel. This indicates that hydroquinone must have been a very active corrosion inhibitor when combined with other inhibitors. Similar trend was observed by Tervusheva *et al.* (2011) and by Gedvillo *et al.* (2019). Eddy *et al.* (2011) reported that 3-tridecene contributed to the inhibition effectiveness of ethanol extract of *Andrographis paniculate* for mild steel in solution of HCl. Awe *et al.* (2015) also identified 3,5-bis(1,1-dimethylethyl)-phenol as active corrosion inhibitors. Others are pentadecanoic acid, a carboxylic acid (Eddy, 2010) and 1-ethenyl-1-methyl-2,4-bis(1-methylethenyl)-cyclohexane (Ameh, 2015).



**Table 8: Frontier molecular orbital energies of active constituents of ethanol extract of PT**

/N	Molecule	E <sub>HOMO</sub> (eV)	E <sub>LUMO</sub> (eV)	ΔE (eV)
1	Hydroquinone	-0.1965	-0.098	0.0985
2	3-tridecene	-0.1836	-0.0499	0.1337
3	3,5-di-tert-butylphenol	-0.1779	-0.0385	0.1394
4	Pentadecanoic acid	-0.1289	-0.1264	0.0025
5	1-ethenyl-1-methyl-2,4-bis(1-methylethenyl)-cyclohexane	-0.1809	-0.0256	0.1553
6	1,1,7-trimethyl-4-methylenedecahydro-1H-cyclopropa[e]azulene	-0.1901	-0.0104	0.1797
7	9-oxa-bicyclo[3,3,1]nona-3,6-dien-2-one	-0.1728	-0.0645	0.1083

Plots of frontier molecular orbital energies of the various components in the ethanol extract of PT leaf (identified by GCMS are presented in Fig. 9 as a function of peak numbers (i.e. peaks 1 to 7).

From the plots, it can be deduced that the contribution of the active components of the plant to corrosion inhibition will followed the order, 1>6>2>5>3>7>4 indicating that the compound identified in peak 1 (hydroquinone) contributed the most while the one peak 4 (1-ethenyl-1-methyl-2,4-bis(1-methylethenyl)-cyclohexane) contributed least. Therefore, corrosion inhibition efficiency of the studied plant extract can be partition to demonstrate the contributions of the various extract based on their frontier molecular energy contributions. Fig 10 shows the HOMO and LUMO diagrams of compounds in ethanol extract of PT leaf. Two sessions were demarcated in each of the diagram, using blue mark to represent electron rich region and yellow to indicate regions where electron density is less. Electron density is seen to concentrates on the hetero atoms and around  $\pi$ -bonds indicating that these compounds have the tendency to donate electron to vacant d-orbital of Fe or accept electron from the ionized Fe metal and form feedback bond (Obi-Egbedi *et al.*, 2011).

In order to qualitatively illustrate the differences in the adsorption behaviour of the molecules in the plant extract, molecular dynamics simulations were carried out using the Forcite quench concept. The structures of the molecules which were optimized with COMPASS forcefield were used for the simulation.

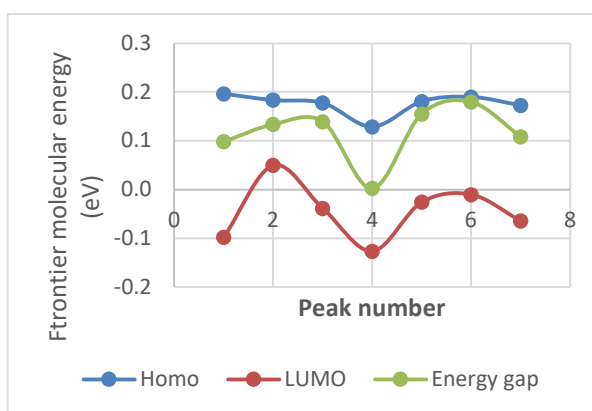


**Fig. 9: Variation of frontier molecular energies of compounds identified by GCMS of ethanol extract of PT leaf**

Solvent and charge effects were neglected and calculations were performed at the metal/vacuum interface in slab. The snapshots of the cross section of the lowest energy adsorption configurations obtained for the compounds in PT are shown in Fig. 11. From the figure, it can be seen that the molecules maintain a flat-lying adsorption orientation on the surface of the metal thereby maximizing contact and enhancing sufficient surface coverage. This parallel adsorption orientation according to Behpour *et al.*, (2011) facilitates interaction of  $\pi$ -electrons and the hetero-atoms in the molecules with the metal surfaces. From the results and findings of the present study, the following conclusions were drawn. Ethanol extract of *Piliostigma thonningii* (PT) leaf is a good adsorption corrosion inhibitor for mild steel in acidic medium.



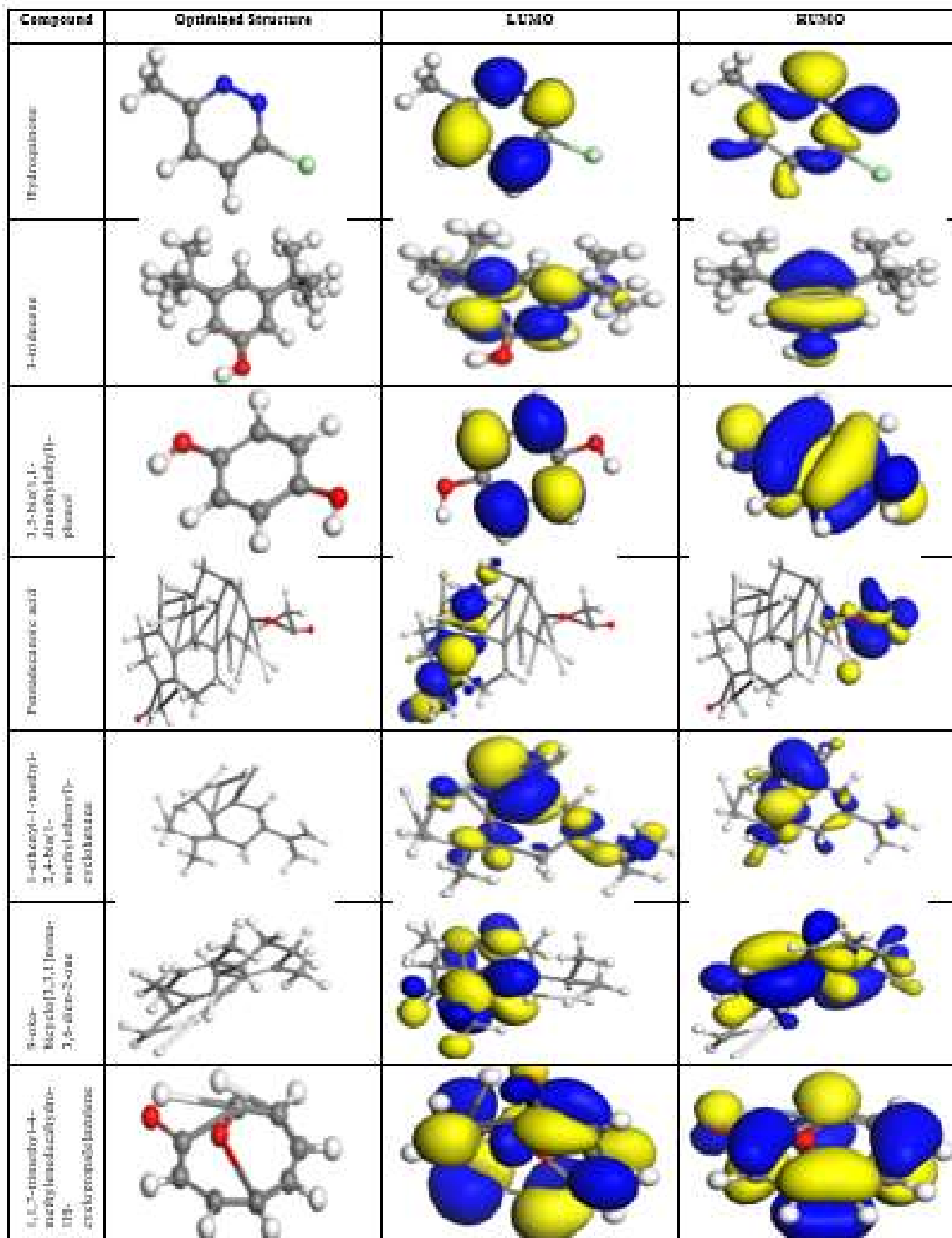


Fig. 10: Optimized structures, HOMO and LUMO molecular orbitals of compounds in ethanol extract of PT leaf (white = H; light gray = C; Red = O; blue = N).



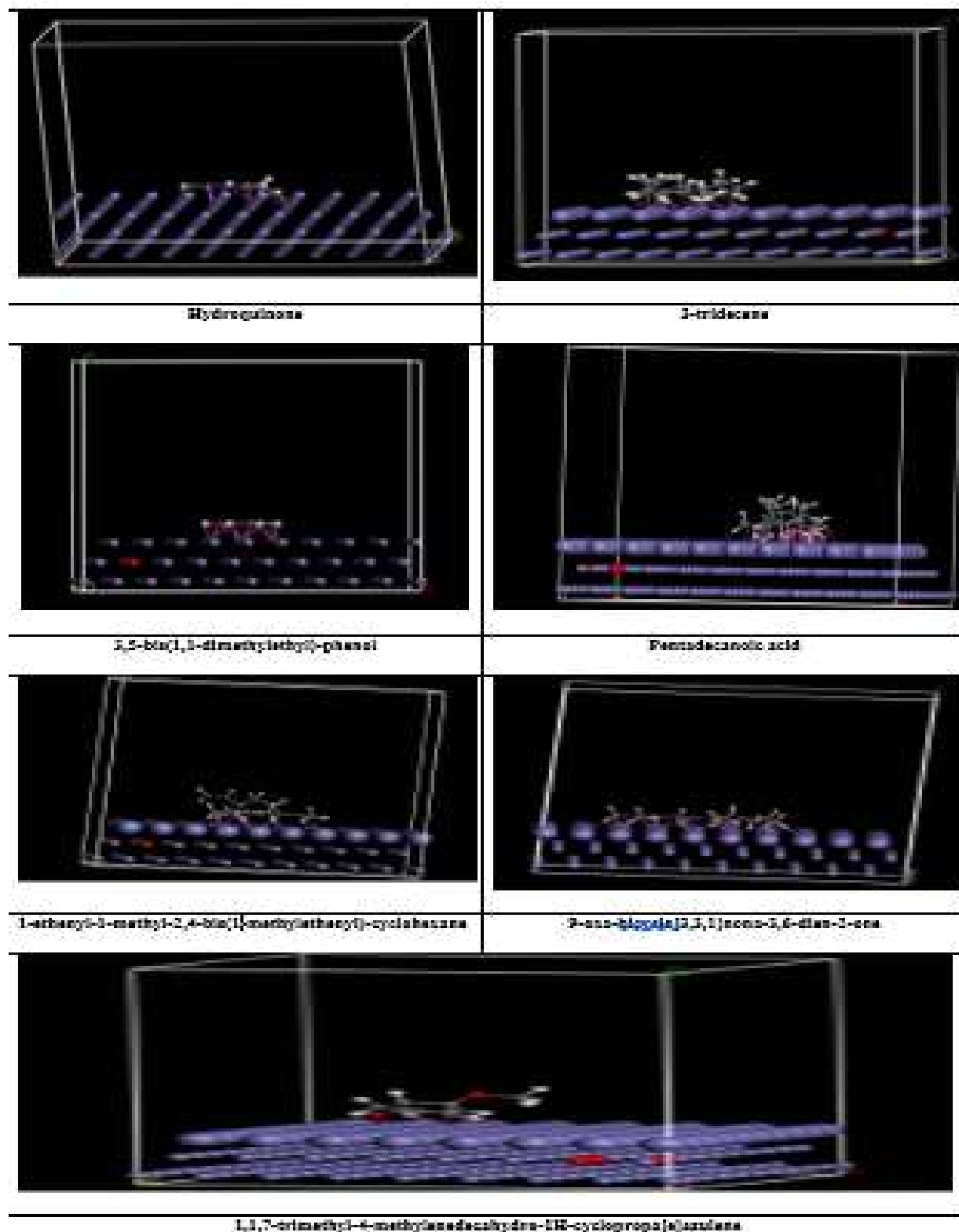


Fig. 11: Adsorption of single molecules of PT extract onto the mild steel surface





#### 4.0 Conclusion

The adsorption of the inhibitor is spontaneous, exothermic and occurred with increasing degree of association. The mechanism of adsorption of the inhibitor is physical adsorption and the adsorption behaviour of the inhibitor best responded to the assumptions of the Langmuir and Frumkin isotherms. Inhibition efficiencies of the inhibitor is affected by temperature, extract concentration and period of contact with the aggressive medium. Quantum chemical calculation and molecular simulation reveal that the inhibition action is due to existent of reactive electron cloud and electron deficiency region, which can simulate adsorption through the formation of coordinate bond or feedback bond. The metal forms parallel stacks on its surface, which accept the inhibitor to be adsorbed and lie on the adsorption sites created on the surface.

#### 4.0References

- Abd El-Rehim, S.S., Hassan, H.H & Amin M.A (2004). Corrosion inhibition study of pure Al and some of its alloys in 1.0 M HCl solution by impedance technique, *Corrosion. Science*, 46 pp 5 – 25.
- Adejo, S.O., Ekwenchi, M.M., Momoh, F. & Odiniya, E. (2012). Adsorption characterization of ethanol extract of leaves of *Portulaca oleracea* as green corrosion inhibitor for corrosion of mild steel in sulphuric acid medium. *International Journal of Modern Chemistry*, 1, 3, pp. 125-134.
- Akalezi, C.O., Enenebaku, C.K. & Oguzie, E.E. (2012). Application of aqueous extracts of coffee senna for control of mild steel corrosion in acidic environments. *International Journal of Industrial Chemistry*, 3, pp. 13-25
- Akinbulumo, O. A., Odejobi, O. J. & Odekanle, E. K. (2020). Thermodynamics and adsorption study of the corrosion inhibition of mild steel by *Euphorbia heterophylla L.* extract in 1.5 M HCl. *Results in Materials*, 5, <https://doi.org/10.1016/j.rinma.2020.100074>
- Ameh, P. O (2018). Electrochemical and computational study of gum *exudates* from *Canarium schweinfurthii* as green corrosion inhibitor for mild steel in HCl solution, *Journal of Taibah University of Science*. 12(6), pp 783 – 795.
- Ameh, P. O. & Eddy, N. O. (2014). *Commiphora pedunculata* gum as a green inhibitor for the corrosion of aluminum alloy in 0.1 M HCl. *Research in Chemical Intermediates*, 40, 8, pp. 2641-2649
- Ameh, P. O. (2015). A Comparative Study of the Inhibitory Effect of Gum Exudates from *Khaya senegalensis* and *Albizia ferruginea* on the Corrosion of Mild Steel in Hydrochloric Acid Medium. *International Journal of Metals*, 2015, <http://dx.doi.org/10.1155/2015/824873>.
- Anand, B. & Chitra, S. (2020). Adsorption studies on the inhibition of the corrosion of mild steel in 2 M NaCl by tetracycline and neomycin trisulphate drugs. *Communication in Physical Sciences*, 5, 2, pp 1-7.
- Arthur, D. E. (2020). Computational and experimental study on corrosion inhibition potential of the synergistic 1:1 combination of Arabic and cashew gum on mild steel. *Petroleum Research*, <https://doi.org/10.1016/j.ptlrs.2020.01.002>.
- ASTM Practice Standard G-31 (2004). Standard Practice for Laboratory Immersion Corrosion Testing of Metals, ASTM International, West Conshohocken, PA, USA.
- Awe, F. E., Abdulwahab, M. & Otaru, H. A. (2019). Adsorptive studies of the inhibitive properties of ethanolic extracts of *Parinari polyandra* on mild steel in acidic media, *Communication in Physical Sciences*, 4(1), pp. 49-57.
- Awe, F. E., Idris, S. O., Abdulwahab, M. & Oguzie, E. E. (2015) Theoretical and experimental inhibitive properties of mild steel in HCl by ethanolic extract of *Boscia senegalensis*, *Cogent Chemistry*, 1:1, 1112676, DOI: 10.1080/23312009.2015.1112676
- Azzan, E. M. S., Abdel-Salam, H. M., Mohamed, R. A., Shaban, S. M. & Shoky, S. A. (2019). *Egyptian Journal of Petroleum*, 27(4) pp. 897-910.
- Banumathi, N., Subhashini, S. & Rajalakshmi, R. (2010). Polyethelene glycol-anthranilic acid composite as corrosion inhibitor for mild steel in acid medium, *Electronic Journal of Chemistry* 7(1), pp 67 – 72.
- Banumathi, N., Subhashini, S. & Rajalakshmi, R. (2010). Polyethelene glycol-anthranilic acid composite as corrosion inhibitor for mild steel in



- acid medium, *Electronic Journal of Chemistry* 7(1), pp 67 – 72.
- Behpour, M.; Ghoreishi, S.M.; Khayatkashani, M. & Soltani, N. (2011). The effect of two oleo-gum resin exudate from *Ferula assa foetida* and *Dorema ammoniacum* on mild steel corrosion in acidic media. *Corrosion Science*, 53, pp 2489 – 2501.
- Benabdellah, M., Touzani, R., Aouniti, A., Dafali, A., El-Kadiri, S. & Hammouti, B (2007). Inhibitive action of some bipyrazolic compounds on the corrosion of steel in 1 M HCl Part I: Electrochemical study, *Material Chemistry and Physics*, 105, pp 373 – 379.
- Burkill, H. M. (1995). The useful plants of West Tropical Africa. 2 Edn., Royal Botanic Garden Kew, pp. 146-149
- Eddy, N. O, Awe, F. E., Siaka, A., Magaji, L. & Ebenso, E. E. (2011). Chemical information from GC-MS studies of ethanol extract of *Andrographis paniculata* and their corrosion inhibition potentials on mild steel in HCl solution. *International Journal of Electrochemical Sciences*, 6, pp. 4316-4328
- Eddy, N. O. & Ebenso, E. E. (2008). Adsorption and inhibitive properties of ethanol extract of *Musa sapientum* peels as a green corrosion inhibitor for mild steel in H<sub>2</sub>SO<sub>4</sub>. *African Journal of Pure and Applied Chemistry*, 2, 6, pp 1-9.
- Eddy, N. O. & Ita, B. I. (2011). Experimental and theoretical studies on the inhibition potentials of some derivatives of cyclopenta-1,3-diene for the corrosion of mild steel in HCl. *International Journal of Quantum Chemistry*, 111, 14, 3456-3474.
- Eddy, N. O. & Odiongenyi, A. O. (2010). *Corrosion inhibition and adsorption properties of ethanol extract of Heinsia crinata on mild steel in H<sub>2</sub>SO<sub>4</sub>*. *Pigment and Resin Technology*, 38, 5, pp.288-295,
- Eddy, N. O. (2009). Inhibitive and adsorption properties of ethanol extract of *Colocasia esculenta* leaves for the corrosion of mild steel in H<sub>2</sub>SO<sub>4</sub>. *International Journal of Physical Sciences*, 3, 2, pp. 1-7.
- Eddy, N. O. (2010). Theoretical study on some amino acids and their potential activity as corrosion inhibitors for mild steel in HCl. *Molecular Simulation*, 35(5) pp 354-363
- Eddy, N. O. & Ebenso, E. E. (2010). Corrosion inhibition and adsorption properties of ethanol extract of *Gongronema latifolium* on mild steel in H<sub>2</sub>SO<sub>4</sub>. *Pigment and Resin Technology*. 42(7), pp 1029-1032.
- Eddy, N. O., Ameh, P. O., Gimba, C. E & Ebenso, E. E. (2013). Rheological Modelling, surface morphology and physicochemical properties of *Anogeissus leiocarpus* gum. *Asian Journal of chemistry*, 25, 3, pp. 1666-167283.
- Eddy, N. O., Awe, F. E., Gimba, C. E., Ibisi, N. & Ebenso, E. E. (2011). QSAR, experimental and computational chemistry simulation studies on the inhibition potentials of some amino acids for the corrosion of mild steel in 0.1 M HCl. *International Journal of Electrochemical Science* 6, pp 931-957
- Eddy, N. O., Awe, F. E., Siaka, A. A., Magaji, L. & Ebenso, E. E. (2011). Chemical information from GCMS studies of ethanol extract of *Andrographis paniculate* and their corrosion inhibition potentials on mild steel in HCl solution. *International Journal of Electrochemical Science*, 6, pp. 4316-4328.
- Eddy, N. O., Ekwumengbo, P. A. & Mamza, P. A. P. (2009a). Ethanol extract of *Terminalia catappa* as a green inhibitor for the corrosion of mild steel in H<sub>2</sub>SO<sub>4</sub>. *Green Chemistry Letters and Review*, 2(4): 223-231.
- Eddy, N. O., Ita, B. I., Dodo, S. N. & Paul, E. D. (2011). Inhibitive and adsorption properties of ethanol extract of *Hibiscus sabdariffa* calyx for the corrosion of mild steel in 0.1 M HCl. *Green Chemistry Letters and Review*, 5, 1, pp. 43-53.
- Eddy, N. O., Odoemelam, S. A. & Odiongenyi, A. O. (2009b). Ethanol extract of *Musa species* peel as a green corrosion inhibitor for mild steel: kinetics, adsorption and thermodynamic considerations. *Electronic Journal of Environmental, Agriculture and Food Chemistry*, 8, 4, pp. 243-255.
- Eddy, N. O., Odoemelam, S. A. & Odiongenyi, A. O. (2009c). Inhibitive, adsorption and synergistic studies on ethanol extract of *Gnetum africana* as green corrosion inhibitor for mild steel in H<sub>2</sub>SO<sub>4</sub>. *Green Chemistry Letters and Review*. 2 (2), pp 111-119.
- Edeoga, H. O., Okwu, D. E., & Mbaebie, B. O. (2005). Phytochemical constituents of some



- Nigerian medicinal plants. *African Journal of Biotechnology*, 4, pp 685-688.
- Gedvillo, I. A., Zhmakina, A. S., Andrew, N. N. & Vesely, S. S. (2019). Effect of hydroquinone and pyrocatechin on the corrosion and electrochemical behaviour of steel in a model concrete pore liquid. *International Journal of Corrosion and Scale Inhibition*, 8, 3, pp. 560-572.
- Hassan, B. O. & Sadek, S. A. (2014). The effect of temperature and hydrodynamics on carbon steel corrosion and its inhibition in oxygenated acid – salt solution, *Journal of Industrial and Engineering Chemistry*, 20(1) pp 297 – 307.
- Jimoh, F. O. & Oladiji A. T. (2005). Preliminary studies on *Piliostigma thonningii* seeds: Preliminary analysis, mineral composition and phytochemical screening. *African Journal of Biotechnology*, 4, pp 1439-1442.
- Karunanithi, B. T. & Chellappa, J. (2019). Adsorption and inhibition properties of *Tephrosia Purpurea* as corrosion inhibitor for mild steel in sulphuric acid solution. *Journal of Dispersion Science and Technology*, 40,10, pp.1441-1450.
- Khalil, N. (2003). Quantum chemical approach of corrosion inhibition, *Electrochim. Acta*. 48 pp 2635–2640.
- Kobe, H. I., Abdulrhman, A. S., Ismail, M. & Mohammed, I. A. (2011). Corrosion inhibition and adsorption characteristics of camel foot leaves extracts on mild steel in hydrochloric acid solution. *Nigerian Journal of Technology Research*, 12, 1, Doi: 10.4314/njtr.v12i1.5.
- Lebrini, M. Robert, F., Lecante, A. & Ross, C. (2010). Corrosion inhibition of C38 steel in 1M hydrochloric acid medium by alkaloids extract from *Annonasqu amosa*, *Journal of Materials Engineering Performance*, 22, pp. 3792–3800.
- Loto, C. A., Joseph, O. O., Loto, R. T. & Popoola, A. P. I. (2014). Corrosion inhibitive behaviour of *Camellias Sinensis* on aluminum alloy in H<sub>2</sub>SO<sub>4</sub>, *International Journal of Electrochemical Science*, 9, pp 1221 – 1231.
- Momoh-Yahaya, H., Eddy, N. O., Iyun, J. F., Gimba, C. E. & Oguzie, E. E. (2014). Inhibitive and Adsorptive Behaviour of Guanine on Corrosion of Mild Steel in 0.1 M HCl and H<sub>2</sub>SO<sub>4</sub>, *International Journal of Modern Chemistry*, 2(3), pp 127 – 142.
- Monika, W.A & Dubey, D. (2005). Inhibition of acid corrosion of mild steel with 1,3-diaminopropane, *Journal of Corrosion Science and Engineering*, 7(23), pp 20 – 31.
- Nwosu, O.F. Nnanna, L.A. & Okeoma, K. B. (2013): Corrosion Inhibition for Mild Steel in 0.5 M H<sub>2</sub>SO<sub>4</sub> solution using *Achyranthes aspera* L. leaf extract. *African Journal of Pure and Applied Chemistry*, 7, 2, pp 56-60.
- Obi-Egbedi, N. O., Obot, I. B., El-Khaiary, M. I., Umoren, S. A. & Ebenso, E. E. (2011). Computational Simulation and statistical analysis on the relationship between corrosion inhibition efficiency and molecular structure of some phenanthroline derivatives on mild steel surface, *International Journal of Electrochemical Science*, 6, pp 5649 – 5675
- Odoemelam, S. A., Ekanem, U. I. & Ekuma, F. K. (2019). Inhibition of corrosion of mild steel in hydrochloric acid solution by Schiff base derived from benheric and linoleic acids. *Communication in Physical Sciences*, 4, 1, pp. 58-66.
- Oguzie, E. E. (2008). Corrosion inhibitive effect and adsorption behaviour of Hibiscus sabdariffa extract on mild steel in acidic media. *Portugaliae Electrochimica Acta*, 26, pp 303-314.
- Onen, A. I., Buba, J., & Apagu, D. A. (2017). Electrochemical analysis of *Piliostigma thonningii* (monkey bread) leaf extract as corrosion inhibitor of aluminum in alkaline Medium. <https://www.semanticscholar.org/paper/Electrochemical-Analysis-of-Piliostigma-thonningii-Onen-Buba/ae58cf0cc5c08dd50a42afced9b9d542b57c5d09>
- Otieno-Alego, V., Hope, G. A., Flitt, H. J. & Schweinsberg, D. P. (1993). The effect of hydroquinone and methoxypropylamine on the pitting corrosion behaviour of A-470 low alloy turbine disc steel. *Corrosion Science*, 34, 8, pp. 1289-1297
- Quraishi, M. A & Singh, A. K. (2010). Piroxicam; A novel corrosion inhibitor for mild steel corrosion in HCl acid solution, *Journal of Materials and Environmental Science*, 1, 2, pp 101 – 110.



- Saraswat, V, & Yadav, M. (2020). Computational and electrochemical analysis on quinoxalines as corrosion inhibitors for mild steel in acidic medium. *Journal of Molecular Liquids*, 297, 1,111993.  
<https://doi.org/10.1016/j.molliq.2019.111883>
- Sherine, B., Nasser, A. J. A. & Rajendran, S. (2010). Inhibitive action of hydroquinone-Zn<sup>2+</sup> system in controlling the corrosion of carbon steel in well water. *International Journal of Engineering Science and Technology*, 24, 4, pp. 341-257.
- Teryusheva, S. A., Beloglazov, G. S., & Beloglazov, S. M. (2011). Experimental and quantum chemical study of quinone derivatives as inhibitors of corrosion and hydrogen absorption by steel. *Solid State Phenomena*, 183, pp. 249–255.
- Umoren, S. A., Obot, I. B. & Ebenso, E. E. (2008). Corrosion inhibition of aluminum using exudate gum from *Pacchylobus edulis* in the presence of halide ions in HCl. *Electronic Journal of Chemistry*, 5, 2, pp 355-364.
- Yinusa, I & Raphael, J. O. (2020). Phytochemical screening, GCMS and FTIR analysis of ethanol extract of *Pilostigma thionningii* (schum Milne-Redth) leaf. *Communication in Physical Sciences*, 5, 1, 22-28
- Zhang, Q. B. & Hua, Y. X. (2009). Corrosion inhibition of mild steel by alkylimidazolium ionic liquids in hydrochloric acid, *Electrochemical Acta*, 54, pp 1881 – 1887.

